Intelligent Systems with Applications 19 (2023) 200243

Contents lists available at ScienceDirect

Intelligent Systems with Applications

journal homepage: www.journals.elsevier.com/intelligent-systems-with-applications

A neuro Meyer wavelet neural network procedure for solving the nonlinear Leptospirosis model

Zulqurnain Sabir [a,b], Muhammad Asif Zahoor Raja [c], Mohamed R. Ali [d,*], R. Sadat [e], Irwan Fathurrochman [f], Rafaél Artidoro Sandoval Núñez [g], Shahid Ahmad Bhat [h]

[a] Department of Mathematics and Statistics, Hazara University, Mansehra, Pakistan
[b] Department of Computer Science and Mathematics, Lebanese American University, Beirut, Lebanon
[c] Future Technology Research Center, National Yunlin University of Science and Technology, 123 University Road, Section 3, Douliou, Yunlin 64002, Taiwan, R.O.C.
[d] Faculty of Engineering and Technology, Future University in Egypt New Cairo 11835, Egypt
[e] Department of Mathematics, Faculty of Engineering, Zagazig University, Zagazig, Egypt
[f] Department of Islamic Educational Management, Institute Agama Islam Negeri Curup, Rejang Lebong, Indonesia
[g] Universidad Nacional Autónoma de Chota, Cajamarca, Perú
[h] LUT Business School, LUT University, P.O. Box 20, FIN-53851 Lappeenranta, Finland

ARTICLE INFO

Keywords:
Mathematical model
Leptospirosis
Wavelet
Genetic algorithm
Neural networks
Active set

ABSTRACT

The aim of such work is to design a Meyer wavelet neural network (WNN) for solving the mathematical form of the Leptospirosis disease model (LDM). The global and local search optimization schemes based on the genetic algorithm (GA) and active-set algorithm (ASA) are used in this study. Leptospirosis is an infection spread by rodents, which is found in the world and causes fatalities in humans. The mathematical LDM model form consists of susceptible-infected-recovered (SIR), which is based on the disease spread processes. A fitness function is designed by using the mathematical LMD and then optimized by the hybridization of the GAASA. For the correctness, and capability of the Meyer WNN along with the procedures of GAASA, the comparison of the obtained and reference results is provided. Moreover, the reducible absolute error provides the efficiency of the proposed Meyer WNN along with the procedures of GAASA. The statistical observations are also provided to authenticate the convergence of the stochastic Meyer WNN along with the procedures of GAASA.

1. Introduction

There are various mathematical models that are based on the system of differential equations. Most of these diseased based differential systems perform the system of first order differential equations. To mention few of them are monkeypox transmission system (Americo et al., 2023, Peter et al., 2021), influenza disease model (Sabir et al., 2022), prey-predator system (Umar et al., 2019), water population model (Sabir et al., 2023), HIV model (Umar et al., 2020), susceptible, infected and quarantine differential model (Bhadauria et al., 2021) and nervous stomach model (Guerrero Sánchez et al., 2020). One of the main factors for identifying the most effective ways to prevent or reduce the Leptospirosis and anticipate its potential manifestations is the use of mathematical models (Khan et al., 2021). The scientists have examined a number of differential systems to identify the dynamical shapes of both people and rat populations. Khan et al. (2016) studied the dynamical form of the Leptospirosis through the saturated rate, which performs the reduction in the susceptible population based on the operative relationship together with the infected people and vectors. Kongnuy (2012) designed a mathematical formulation for the Leptospirosis spreading that is a connection between the populations of vector and humans. The Leptospirosis control is possible to decrease the spreading rate based on the vectors of infected to susceptible. The proposed model simulation rate through the rate of infection is 0.83, which performs the reduction in the spread of Leptospirosis. Some related world spreading diseases are cited in Sabir et al. (2021), Sánchez et al. (2020) and Umar et al. (2020).

In the past few years, mathematics has been used to analyze the global spread of virus mechanism (Keeling, 2001). Many diseases, including the dengue, coronavirus, hantavirus, malaria, and leptospirosis are prevalent worldwide (Sabir et al., 2021, Umar et al., 2020). Only a small number of illnesses that spread from to another individual are categorized as transmissible diseases, whereas illnesses that are

* Corresponding author.
E-mail address: mohamed.reda@bhit.bu.edu.eg (M.R. Ali).

https://doi.org/10.1016/j.iswa.2023.200243
Received 7 January 2023; Received in revised form 4 May 2023; Accepted 27 May 2023
Available online 19 June 2023

typically brought through the or genetic or environmental factors, which are known as harmless viruses (Keeling and Rohani, 2011). Leptospirosis is recognized as a microbial or animal disease that govern through the infection and prey the humans (Thayaparan et al., 2013). Leptospira dissemination occurs because of host feces getting into water or mud. Leptospira-carrying hosts do not experience any physical harm (Lim et al., 2011). Humans may contract infections if they incur injuries to their outer layers that encounter the urine-contaminated food and water (Bhalraj and Azmi, 2019). The epidemics of Leptospirosis occur rapidly when people consume contaminated water, such as flooding (Triampo et al., 2007). The rate of disease spread among the people is quite sporadic (El-Shahed, 2014). Typically, the main resources of the bacteria are sheep, dogs, raccoons, rats, goats, mice, pigs, horses, and cattle (Goh et al., 2019).

The present study performs the design of a Meyer wavelet neural network (WNN) together with the global and local search optimization schemes based on the genetic algorithm (GA) and active-set algorithm (ASA) to solve the mathematical form of the Leptospirosis disease model (LDM). The LDM consists of susceptible, infected, and recovered (SIR), which includes the vector (rat) and the population of human, which is shown as (Bhalraj et al., 2021):

$$\begin{cases} \dfrac{dS_h}{dx} = \theta_h R_h(x) - (\mu_h + \beta_h I_r(x))S_h(x) + A, \\ \dfrac{dI_h}{dx} = \beta_h I_r(x)S_h(x) - (\mu_h + r_h + \delta_h)I_h(x), \\ \dfrac{dR_h}{dx} = -(\theta_h + \mu_h)R_h(x) + r_h I_h(x), \\ \dfrac{dS_r}{dx} = -r(_r + \beta_r I_h(x))S_r(x) + B, \\ \dfrac{dI_r}{dx} = -(\delta_r + r_r)I_r(x) + \beta_r I_h(x)S_r(x), \end{cases} \tag{1}$$

Where S_h and S_r are the susceptible human and rat, R_h is the recovered human, while I_h and I_r are the infected human and rat, A and B are the recruitment rate of people and rat, μ_h and r_r are the human and rat natural death rate, β_h and β_r are the Leptospirosis transmission rate from infected rat to susceptible people and infected to susceptible rat, r_h presents the recovered rate in humans, θ_h presents the immune rate in people to sceptible again, δ_h rate of infected people that die with Leptospirosis and δ_r is the rate of infection that becomes the reason of rat's death.

The above model given in system (1) has been numerically performed by designing the stochastic procedure of Meyer WNN along with the optimization of GAASA for presenting the solutions of LDM. The stochastic based applications have been widely used in recent decades to solve various differential models, some of them are eye surgery model (Umar, 2019), periodic model (Sabir, 2020), food chain model (Sabir, 2022) and thermal explosion system (Sabir, 2022). By keeping in view of the significance of these stochastic applications, the authors are motivated to present the solutions of the LDM by applying the procedures of Meyer WNN along with the optimization of GAASA.

The other sections of this study are provided as: The methodology is presented in Sect 2, the results are provided in Sect 3, while the conclusions are shown in the last Sect.

2. Methodology

The Meyer WNNs together with the GAASA optimization is presented for the numerical solutions of the LDM.

2.1. Proposed Meyer WNN-GAASA

The representations based on the LDM are designed as:

$$[\widehat{S}_h, \widehat{I}_h, \widehat{R}_h, S_r, I_r] = \begin{bmatrix} \sum_{k=1}^{y} z_{S_h,k} U\left(w_{S_h,k}x + m_{S_h,k}\right), \sum_{k=1}^{y} z_{I_h,i} U\left(w_{I_h,k}x + m_{I_h,k}\right), \\ \sum_{k=1}^{y} z_{R_h,k} U\left(w_{R_h,k}x + m_{R_h,k}\right), \sum_{k=1}^{y} z_{S_h,i} U\left(w_{S_r,k}x + m_{S_r,k}\right), \\ \sum_{k=1}^{y} z_{I_r,k} U\left(w_{I_r,k}x + m_{I_r,k}\right), \end{bmatrix}, \tag{2}$$

$$\begin{aligned} &\left[\widehat{S}_h^{(n)}, \widehat{I}_h^{(n)}, \widehat{R}_h^{(n)}, S_r^{(n)}, I_r^{(n)}\right] \\ &= \begin{bmatrix} \sum_{k=1}^{y} z_{S_h,k} U^{(n)}\left(w_{S_h,k}x + m_{S_h,k}\right), \sum_{k=1}^{y} z_{I_h,i} U^{(n)}\left(w_{I_h,k}x + m_{I_h,k}\right), \\ \sum_{k=1}^{y} z_{R_h,k} U^{(n)}\left(w_{R_h,k}x + m_{R_h,k}\right), \sum_{k=1}^{y} z_{S_h,i} U^{(n)}\left(w_{S_r,k}x + m_{S_r,k}\right), \\ \sum_{k=1}^{y} z_{I_r,k} U^{(n)}\left(w_{I_r,k}x + m_{I_r,k}\right), \end{bmatrix}, \end{aligned}$$

where the proposed results are $\widehat{S}_h$, $\widehat{I}_h$, $\widehat{R}_h$, S_r and I_r. The unknown weights $W = [W_{S_h}, W_{I_h}, W_{R_h}, W_{S_h}, W_{I_h}]$ are provided as:

$W_{S_h} = [z_{S_h}, \omega_{S_h}, m_{S_h}]$, $W_{S_h} = [z_{I_h}, \omega_{I_h}, m_{I_h}]$, $W_{R_h} = [z_{R_h}, \omega_{R_h}, m_{R_h}]$, $W_{S_h} = [z_{S_h}, \omega_{S_h}, m_{S_h}]$ and $W_{S_h} = [z_{I_h}, \omega_{I_h}, m_{I_h}]$, where

$$\begin{aligned} &z_{S_h} = \left[z_{S_h,1}, z_{S_h,2}, \ldots, z_{S_h,y}\right], \quad z_{I_h} = \left[z_{I_h,1}, z_{I_h,2}, \ldots, z_{I_h,y}\right], \quad z_{R_h} = \left[z_{R_h,1}, z_{R_h,2}, \ldots, z_{R_h,y}\right], \\ &z_{S_r} = \left[z_{S_r,1}, z_{S_r,2}, \ldots, z_{S_r,y}\right], \quad z_{I_r} = \left[z_{I_r,1}, z_{I_r,2}, \ldots, z_{I_r,y}\right], \quad w_{S_h} = \left[w_{S_h,1}, w_{S_h,2}, \ldots, w_{S_h,y}\right], \\ &w_{I_h} = \left[w_{I_h,1}, w_{I_h,2}, \ldots, w_{I_h,y}\right], \quad w_{R_h} = \left[w_{R_h,1}, w_{R_h,2}, \ldots, w_{R_h,y}\right], \quad w_{S_r} = \left[w_{S_r,1}, w_{S_r,2}, \ldots, w_{S_r,y}\right], \\ &w_{I_r} = \left[w_{I_r,1}, w_{I_r,2}, \ldots, w_{I_r,y}\right], \; m_{S_h} = \left[m_{S_h,1}, m_{S_h,2}, \ldots, m_{S_h,y}\right], \; m_{I_h} = \left[m_{I_h,1}, m_{I_h,2}, \ldots, m_{I_h,y}\right], \\ &m_{R_h} = \left[m_{R_h,1}, m_{R_h,2}, \ldots, m_{R_h,y}\right], \; m_{S_r} = \left[m_{S_r,1}, m_{S_r,2}, \ldots, m_{S_r,y}\right], \; m_{I_r} = \left[m_{I_r,1}, m_{I_r,2}, \ldots, m_{I_r,y}\right]. \end{aligned}$$

The Meyer WNNs together with the GAASA has never been applied before to solve the LDM, the mathematical form of the Meyer function is presented as:

$$U(x) = x^4\left(35 - 84x + 70x^2 - 20x^3\right) \tag{3}$$

System (2) using the above Eq. (3) becomes as:

$$[\widehat{S}_h,\ \widehat{I}_h,\ \widehat{R}_h, S_r, I_r] = \begin{bmatrix} \sum_{k=1}^{y} z_{S_h,k} \begin{pmatrix} 35\left(w_{S_h,k}x + m_{S_h,k}\right)^4 - 84\left(w_{S_h,k}x + m_{S_h,k}\right)^5 \\ +70\left(w_{S_h,k}x + m_{S_h,k}\right)^6 - 20\left(w_{S_h,k}x + m_{S_h,k}\right)^7 \end{pmatrix}, \\ \sum_{k=1}^{y} z_{I_h,k} \begin{pmatrix} 35\left(w_{I_h,k}x + m_{I_h,k}\right)^4 - 84\left(w_{I_h,k}x + m_{I_h,k}\right)^5 \\ +70\left(w_{I_h,k}x + m_{I_h,k}\right)^6 - 20\left(w_{I_h,k}x + m_{I_h,k}\right)^7 \end{pmatrix}, \\ \sum_{k=1}^{y} z_{R_h,k} \begin{pmatrix} 35\left(w_{R_h,k}x + m_{R_h,k}\right)^4 - 84\left(w_{R_h,k}x + m_{R_h,k}\right)^5 \\ +70\left(w_{R_h,k}x + m_{R_h,k}\right)^6 - 20\left(w_{R_h,k}x + m_{R_h,k}\right)^7 \end{pmatrix}, \\ \sum_{k=1}^{y} z_{S_r,k} \begin{pmatrix} 35\left(w_{S_r,k}x + m_{S_r,k}\right)^4 - 84\left(w_{S_r,k}x + m_{S_r,k}\right)^5 \\ +70\left(w_{S_r,k}x + m_{S_r,k}\right)^6 - 20\left(w_{S_r,k}x + m_{S_r,k}\right)^7 \end{pmatrix}, \\ \sum_{k=1}^{y} z_{I_r,k} \begin{pmatrix} 35\left(w_{I_r,k}x + m_{I_r,k}\right)^4 - 84\left(w_{I_r,k}x + m_{I_r,k}\right)^5 \\ +70\left(w_{I_r,k}x + m_{I_r,k}\right)^6 - 20\left(w_{I_r,k}x + m_{I_r,k}\right)^7 \end{pmatrix}, \end{bmatrix}, \tag{4}$$

$$[\widehat{S}_h^{'},\ \widehat{I}_h^{'},\ \widehat{R}_h^{'},\ \widehat{S}_r^{'}, \widehat{I}_r^{'}] = \frac{d}{dx} \begin{bmatrix} \sum_{k=1}^{y} z_{S_h,k} \begin{pmatrix} 35\left(w_{S_h,k}x + m_{S_h,k}\right)^4 - 84\left(w_{S_h,k}x + m_{S_h,k}\right)^5 \\ +70\left(w_{S_h,k}x + m_{S_h,k}\right)^6 - 20\left(w_{S_h,k}x + m_{S_h,k}\right)^7 \end{pmatrix}, \\ \sum_{k=1}^{y} z_{I_h,k} \begin{pmatrix} 35\left(w_{I_h,k}x + m_{I_h,k}\right)^4 - 84\left(w_{I_h,k}x + m_{I_h,k}\right)^5 \\ +70\left(w_{I_h,k}x + m_{I_h,k}\right)^6 - 20\left(w_{I_h,k}x + m_{I_h,k}\right)^7 \end{pmatrix}, \\ \sum_{k=1}^{y} z_{R_h,k} \begin{pmatrix} 35\left(w_{R_h,k}x + m_{R_h,k}\right)^4 - 84\left(w_{R_h,k}x + m_{R_h,k}\right)^5 \\ +70\left(w_{R_h,k}x + m_{R_h,k}\right)^6 - 20\left(w_{R_h,k}x + m_{R_h,k}\right)^7 \end{pmatrix}, \\ \sum_{k=1}^{y} z_{S_r,k} \begin{pmatrix} 35\left(w_{S_r,k}x + m_{S_r,k}\right)^4 - 84\left(w_{S_r,k}x + m_{S_r,k}\right)^5 \\ +70\left(w_{S_r,k}x + m_{S_r,k}\right)^6 - 20\left(w_{S_r,k}x + m_{S_r,k}\right)^7 \end{pmatrix}, \\ \sum_{k=1}^{y} z_{I_r,k} \begin{pmatrix} 35\left(w_{I_r,k}x + m_{I_r,k}\right)^4 - 84\left(w_{I_r,k}x + m_{I_r,k}\right)^5 \\ +70\left(w_{I_r,k}x + m_{I_r,k}\right)^6 - 20\left(w_{I_r,k}x + m_{I_r,k}\right)^7 \end{pmatrix}, \end{bmatrix}, \tag{4}$$

A fitness function based on the LDM is provided as:

$$E_f = \sum_{i=i}^{6} \left(E_f\right)_i \tag{5}$$

$$E_{f-1} = \frac{1}{N}\sum_{r=1}^{N}\left[(\widehat{S}_h^{'})_r - \theta_h\widehat{R}_h + (\mu_h + \beta_h\widehat{I}_r)\widehat{S}_h - A\right]^2, \tag{6}$$

$$E_{f-2} = \frac{1}{N}\sum_{r=1}^{N}\left[(\widehat{I}_h^{'})_r + (r_h + \mu_h + \delta_h)I_h - \beta_h S_h I_r\right]^2, \tag{7}$$

$$E_{f-3} = \frac{1}{N}\sum_{r=1}^{N}\left[(\widehat{R}_h^{'})_r - r_h\widehat{I}_h + (\theta_h + \mu_h)\widehat{R}_h\right]^2, \tag{8}$$

$$E_{f-4} = \frac{1}{N}\sum_{r=1}^{N}\left[(\widehat{S}_r^{'})_r + (\beta_r\widehat{I}_r + r)_r\widehat{S}_r - B\right]^2, \tag{9}$$

$$E_{f-5} = \frac{1}{N}\sum_{r=1}^{N}\left[(\widehat{I}_r^{'})_r - \beta_r(\widehat{S}_h - (r_r + \delta_r))\widehat{I}_r\right]^2, \tag{10}$$

$$E_{f-6} = \frac{1}{5}\left[\left((\widehat{S}_h)_0 - j_1\right)^2 + \left((\widehat{I}_h)_0 - j_2\right)^2 + \left((\widehat{R}_h)_0 - j_3\right)^2 + \left((\widehat{S}_r)_0 - j_4\right)^2 + \left((\widehat{I}_r)_0 - j_5\right)^2\right], \tag{10}$$

2.2. Optimization GAASA

The performances of the optimization by using the GAASA are presented to solve the LDM. Fig. 1 represents the structure of the Mayer WNN-GAASA to solve the LDM.

GA is considered as a global search optimization solver that is applied to solve the models based on the constrained and constrained types through the best results selection. In this work, GA is used to perform the numerical outcomes of the model based on the Leptospirosis. GA is normally implemented to switch the accurate population results for various complicated and stiff models based on the optimal training procedure. To achieve the optimal model performances, it works through the crossover, mutation, and reproduction operatives. Some noteworthy applications of GA are vehicle travel distance (Shanmugasundaram et al., 2019), wellhead back pressure control system (Liang et al., 2020), cancer categorization (Sathya et al., 2022), fault

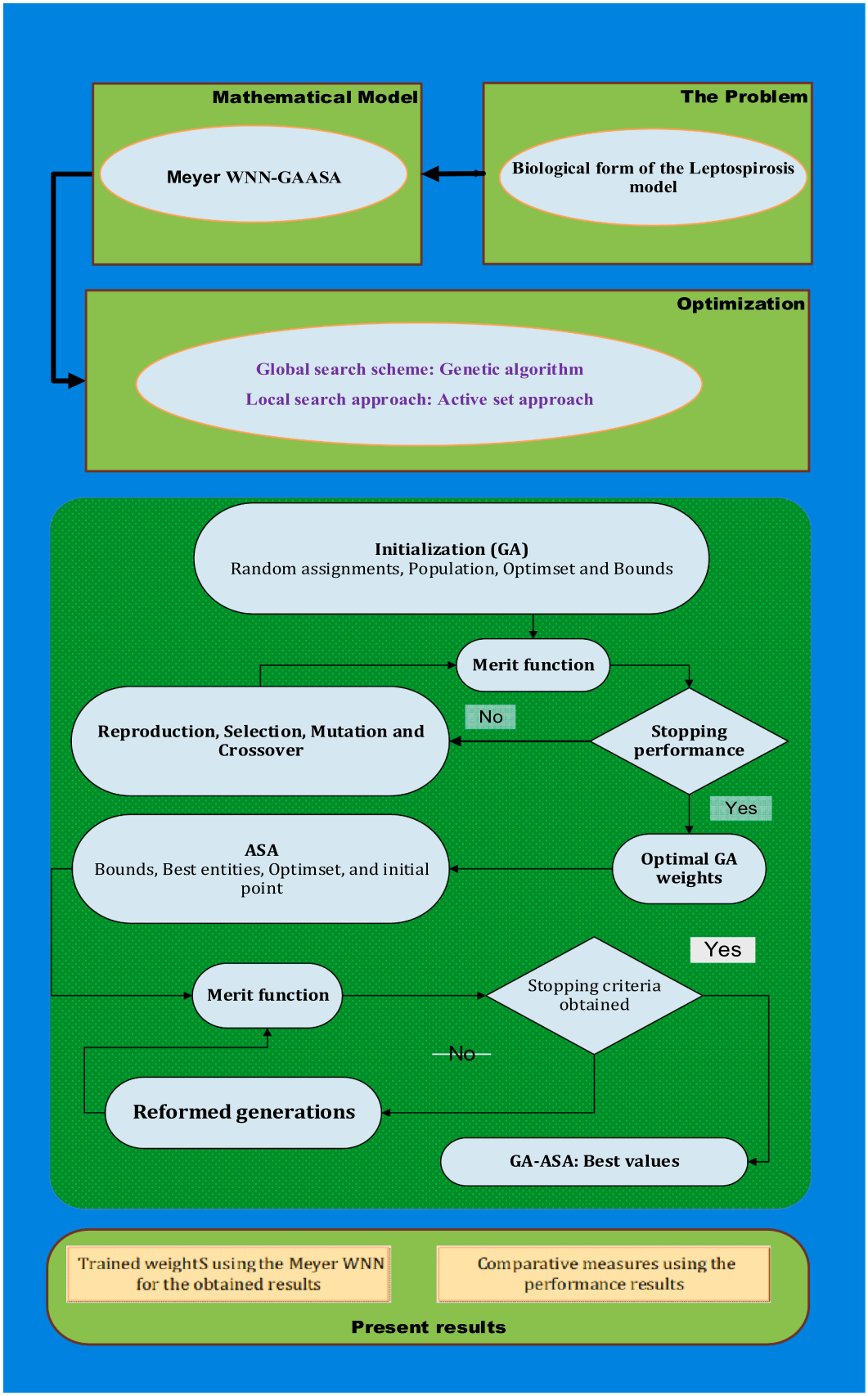

Fig. 1. Designed Meyer WNN-GAASA for solving the LDM.

detection of wind turbines (Khan et al., 2023), cloud service composition optimization (Yang et al., 2019), optimal operation strategy of thermal energy storage tank in combined heat and power units (Wang et al., 2021), fit parameters based on the coronavirus model (Yarsky, 2021), dynamic programming for fuel/emissions reduction (Wang et al., 2021), cluster studies (El-Shorbagy et al., 2019), and fuel cell fault diagnosis (Huo et al., 2022).

ASA is known as an optimization based local search solver, which is generally executed in both systems of constrained and unconstrained networks. It is implemented to present the various intricate and non-stiff models. In recent some decades, it is instigated for pressure-dependent model of water distribution systems (Deuerlein et al., 2019), real-time optimal control systems (Quirynen et al., 2018), American lookback put option pricing (Song et al., 2017), non-smooth contact dynamics (Abide et al., 2021), nonlinear problems with-monotone operators (He and Yang, 2019) and multi-rigid-body dynamic contact problems (Barboteu and Dumont, 2018). The combination of GAASA is applied to control the slowness of the global solver. The process of Meyer WNN along with the optimization of GAASA in Tabulated in Table 1.

2.3. Statistical measures

This part of the study provides the statistical measures using the VAF, semi-interquartile range (S-I-R), and TIC for solving the LDM:

$$\begin{cases} \begin{bmatrix} \mathrm{VAF}_{S_h}, & \mathrm{VAF}_{I_h}, \\ \mathrm{VAF}_{R_h}, & \mathrm{VAF}_{S_r}, \\ \mathrm{VAF}_{I_r} \end{bmatrix} = \begin{bmatrix} \left(1-\frac{\mathrm{var}\left((S_h)_j-(\widehat{S}_h)_j\right)}{\mathrm{var}(S_h)_j}\right)*100, & \left(1-\frac{\mathrm{var}\left((I_h)_j-(\widehat{I}_h)_j\right)}{\mathrm{var}(I_h)_j}\right)*100, \\ \left(1-\frac{\mathrm{var}\left((R_h)_j-(\widehat{R}_h)_j\right)}{\mathrm{var}(R_h)_j}\right)*100, & \left(1-\frac{\mathrm{var}\left((S_r)_j-(\widehat{S}_r)_j\right)}{\mathrm{var}(S_r)_j}\right)*100, \\ \left(1-\frac{\mathrm{var}\left((I_r)_j-(\widehat{I}_r)_j\right)}{\mathrm{var}(I_r)_j}\right)*100, \end{bmatrix}, \end{cases} \tag{11}$$

$$\begin{cases} \mathrm{S}-\mathrm{I}-\mathrm{R}=-\frac{1}{2}(Q_1-Q_3), \\ Q_1, Q_3 = 1^{st}, 3^{rd}\text{quartile}, \end{cases} \tag{12}$$

$$\begin{bmatrix} \mathrm{TIC}_{S_h}, & \mathrm{TIC}_{I_h}, \\ \mathrm{TIC}_{R_h}, & \mathrm{TIC}_{S_r}, \\ \mathrm{TIC}_{I_r} \end{bmatrix} = \begin{bmatrix} \frac{\sqrt{\frac{1}{n}\sum_{i=1}^{n}\left((S_h)_i-(\widehat{S}_h)_i\right)^2}}{\left(\sqrt{\frac{1}{n}\sum_{i=1}^{n}(S_h)_i^2}+\sqrt{\frac{1}{n}\sum_{i=1}^{n}(\widehat{S}_h)_i^2}\right)}, & \frac{\sqrt{\frac{1}{n}\sum_{i=1}^{n}\left((I_h)_i-(\widehat{I}_h)_i\right)^2}}{\left(\sqrt{\frac{1}{n}\sum_{i=1}^{n}(I_h)_r^2}+\sqrt{\frac{1}{n}\sum_{i=1}^{n}(\widehat{I}_h)_i^2}\right)}, \\ \frac{\sqrt{\frac{1}{n}\sum_{i=1}^{n}\left((R_h)_i-(\widehat{R}_h)_i\right)^2}}{\left(\sqrt{\frac{1}{n}\sum_{i=1}^{n}(R_h)_i^2}+\sqrt{\frac{1}{n}\sum_{i=1}^{n}(\widehat{R}_h)_i^2}\right)}, & \frac{\sqrt{\frac{1}{n}\sum_{i=1}^{n}\left((S_r)_i-(\widehat{S}_r)_i\right)^2}}{\left(\sqrt{\frac{1}{n}\sum_{i=1}^{n}(S_r)_i^2}+\sqrt{\frac{1}{n}\sum_{i=1}^{n}(\widehat{S}_r)_i^2}\right)}, \\ \frac{\sqrt{\frac{1}{n}\sum_{i=1}^{n}\left((I_r)_i-(\widehat{I}_r)_i\right)^2}}{\left(\sqrt{\frac{1}{n}\sum_{i=1}^{n}(I_r)_i^2}+\sqrt{\frac{1}{n}\sum_{i=1}^{n}(\widehat{I}_r)_i^2}\right)} \end{bmatrix}, \tag{13}$$

3. Results

The numerical results of the LDM are provided by applying the Meyer WNN along with the optimization of the GAASA. The Eq. (1) is updated by taking the appropriate values is presented as:

$$\begin{cases} \frac{dS_h}{dx} = 0.0067R_h(x) - (0.03 + 0.0098I_r(x))S_h(x) + 1.6, & (S_h)_0 = 100, \\ \frac{dI_h}{dx} = (0.0098S_h(x) - 0.0411)I_h(x), & (I_h)_0 = 20, \\ \frac{dR_h}{dx} = -0.0407R_h(x) + 0.007I_h(x), & (R_h)_0 = 30, \\ \frac{dS_r}{dx} = -(0.17 + 0.078I_h(x))S_r(x) + 1.2, & (S_r)_0 = 50, \\ \frac{dI_r}{dx} = -0.264I_r(x) + 0.078S_r(x)I_h(x), & (I_r)_0 = 10, \end{cases} \tag{14}$$

A merit function is provided as:

$$E_f = \frac{1}{N}\sum_{r=1}^{N}\begin{pmatrix}[\widehat{S}_h^{'} + (0.03 + 0.0098\widehat{I}_h)\widehat{S}_h - 1.6 - 0.0067\widehat{R}_h]^2 \\ +[\widehat{I}_h^{'} - (0.0098\widehat{S}_h - 0.0411)\widehat{I}_h]^2 + [\widehat{R}_h^{'} + 0.0407\widehat{R}_h - 0.007\widehat{I}_h]^2 \\ +[\widehat{S}_r^{'} - 1.2 + (0.17 + 0.078\widehat{I}_h)\widehat{S}_r]^2 + [\widehat{I}_r^{'} - 0.078\widehat{S}_r\widehat{I}_h + 0.0264\widehat{I}_r]^2\end{pmatrix} \\ +\frac{1}{5}\left[\left((\widehat{S}_h)_0 - 100\right)^2 + \left((\widehat{I}_h)_0 - 20\right)^2 + \left((\widehat{R}_h)_0 - 30\right)^2 + \left((\widehat{S}_r)_0 - 50\right)^2 + \left((\widehat{I}_r)_0 - 10\right)^2\right]. \tag{15}$$

The performances based on the optimization of the GAASA to solve the LDM are provided for 10 runs to get the Meyer WNN parameters. The optimal weights are graphically presented in Fig. 2 using the optimization of the GAASA to solve the LDM. The mathematical form of these outcomes is given as:

$$\widehat{S}_h(x) = 15.764\begin{pmatrix}35(-1.833x - 0.2151)^4 - 84(-1.8337x - 0.2151)^5 \\ +70(-1.83x - 0.2151)^6 - 20(-1.833x - 0.2151)^7\end{pmatrix} \\ +2.3945\begin{pmatrix}35(-6.869x - 6.7549)^4 - 84(-6.8690x - 6.7549)^5 \\ +70(-6.86x - 6.754)^6 - 20(-6.8690x - 6.7549)^7\end{pmatrix} \\ +\ldots + 13.485\begin{pmatrix}35(1.9753x + 6.9039)^4 - 84(1.9753x + 6.9039)^5 \\ +70(1.9753x + 6.903)^6 - 20(1.9753x + 6.9039)^7\end{pmatrix}. \tag{16}$$

$$\widehat{I}_h(x) = 5.4265\begin{pmatrix}35(0.9090x + 2.2287)^4 - 84(0.9090x + 2.2287)^5 \\ +70(0.9090x + 2.2287)^6 - 20(0.9090x + 2.228)^7\end{pmatrix} \\ +6.3929\begin{pmatrix}35(1.1902x + 2.1429)^4 - 84(1.1902x + 2.1429)^5 \\ +70(1.190x + 2.1429)^6 - 20(1.1902x + 2.1429)^7\end{pmatrix} \\ +\ldots + 4.6736\begin{pmatrix}35(0.6809x + 1.0950)^4 - 84(0.6809x + 1.0950)^5 \\ +70(0.6809x + 1.095)^6 - 20(0.6809x + 1.0950)^7\end{pmatrix}. \tag{17}$$

$$\widehat{R}_h(x) = 5.2197\begin{pmatrix}35(0.0760x + 1.9765)^4 - 84(0.0760x + 1.9765)^5 \\ +70(0.076x + 1.976)^6 - 20(0.0760x + 1.9765)^7\end{pmatrix} \\ +2.5158\begin{pmatrix}35(-0.052x + 2.5449)^4 - 84(-0.052x + 2.5449)^5 \\ +70(-0.052x + 2.544)^6 - 20(-0.052x + 2.5449)^7\end{pmatrix} \\ +\ldots + 6.2987\begin{pmatrix}35(-0.127x + 1.8212)^4 - 84(-0.127x + 1.8212)^5 \\ +70(-0.127x + 1.8212)^6 - 20(-0.127x + 1.8212)^7\end{pmatrix}. \tag{18}$$

$$\widehat{S}_r(x) = 5.2197\begin{pmatrix}35(8.7162x + 2.8414)^4 - 84(8.7162x + 2.8414)^5 \\ +70(8.7162x + 2.841)^6 - 20(8.7162x + 2.8414)^7\end{pmatrix} \\ +3.4090\begin{pmatrix}35(0.7226x + 3.0054)^4 - 84(0.7226x + 3.0054)^5 \\ +70(0.722x + 3.0054)^6 - 20(0.7226x + 3.0054)^7\end{pmatrix} \\ +\ldots + 8.0987\begin{pmatrix}35(-1.834x + 0.3521)^4 - 84(-1.834x + 0.3521)^5 \\ +70(-1.83x + 0.3521)^6 - 20(-1.834x + 0.3521)^7\end{pmatrix}. \tag{19}$$

$$\widehat{I}_r(x) = -0.091\begin{pmatrix}35(-1.632x + 0.5051)^4 - 84(-1.632x + 0.5051)^5 \\ +70(-1.63x + 0.5051)^6 - 20(-1.632x + 0.5051)^7\end{pmatrix} \\ +0.7234\begin{pmatrix}35(-2.257x - 0.3641)^4 - 84(-2.257x - 0.3641)^5 \\ +70(-2.25x - 0.3641)^6 - 20(-2.257x - 0.3641)^7\end{pmatrix} \\ +\ldots + 0.1846\begin{pmatrix}35(-2.057x - 0.1572)^4 - 84(-2.057x - 0.1572)^5 \\ +70(-2.057x - 0.157)^6 - 20(-2.057x - 0.1572)^7\end{pmatrix}. \tag{20}$$

Fig. 2 presents the optimal weight vectors using the Meyer WNN along with the GAASA for solving the nonlinear dynamics of the LDM. Fig. 2 is drawn on the basis of best weight vectors, which are shown in Eqs. (16) to (20). Fig. 3 shows the comparison performances based on the optimal and reference results that have been performed by using the LDM. The overlapping of both results performs the correctness of the stochastic Meyer WNN along with the GAASA for solving the nonlinear dynamics of the LDM. Fig. 4 presents the values of AE for each dynamic of the LDM using the Meyer WNN along with GAASA. The best AE values of the 1st, 2nd, 3rd, 4th and 5th classes of the LDM are performed as 10^{-05}-10^{-06}, while the mean values of the AE are given as 10^{-04}-10^{-05} for respective cases of the model. These AE-based indications indicate the proposed Meyer WNN along with the GAASA are effective for solving the nonlinear dynamics of the LDM.

Figs. 5 and 6 signify the convergence of TIC and EVAF operator values along with the histograms (H.Gs) using the Meyer WNN-GAASA to solve the nonlinear dynamics of the LDM. These operator values based

Table 1
Optimization using the Meyer WNN-GAASA to solve the LDM.

GA process initiates
- **Inputs:** The chromosome are $W = [W_{S_h}, W_{I_h}, W_{R_h}, W_{S_h}, W_{I_h}]$
- **Population:** The chromosomes set is $W_{S_h} = [z_{S_h}, \omega_{S_h}, m_{S_h}]$, $W_{S_h} = [z_{I_h}, \omega_{I_h}, m_{I_h}]$, $W_{R_h} = [z_{R_h}, \omega_{R_h}, m_{R_h}]$, $W_{S_h} = [z_{S_h}, \omega_{S_h}, m_{S_h}]$ and $W_{S_h} = [z_{I_h}, \omega_{I_h}, m_{I_h}]$
- **Output:** Best global performances are $\boldsymbol{W_{BGA}}$
- **Start point:** For the chromosome's selection, the weight vectors are used.
- **Assessment of fitness:** Calculate fitness (E_F) using the population

• **Stopping standards:** [TolCon/Fun = 10^{-19}], [StallLimit=180], [PopSize=330], [$E_F = 10^{-16}$], and [Generations = 70]

Go to **[storage]**.
- **Ranking:** Rank the weight vector using the population.
- **Storage:** function count, $\boldsymbol{W_{BGA}}$, time, E_F, and iterations.

[GA] process ends

ASA initiates
- **Inputs:** $\boldsymbol{W_{BGA}}$
- **Output:** $\boldsymbol{W_{GAASA}}$ shows the best GA-ASA resutls.
- **Initialize:** Assignments, $\boldsymbol{W_{BGA}}$, and iterations.
- **Terminate:** [E_F=TolFun/Con/X = 10^{-19}], [Iterations = 1000], & [MaxFunEvals= 150000].
- **Fitness performance:** Compute E_F and weight vectors.
- **Accumulate:** Transmute function counts, $\boldsymbol{W_{GAASA}}$, E_F, and time.

ASA End

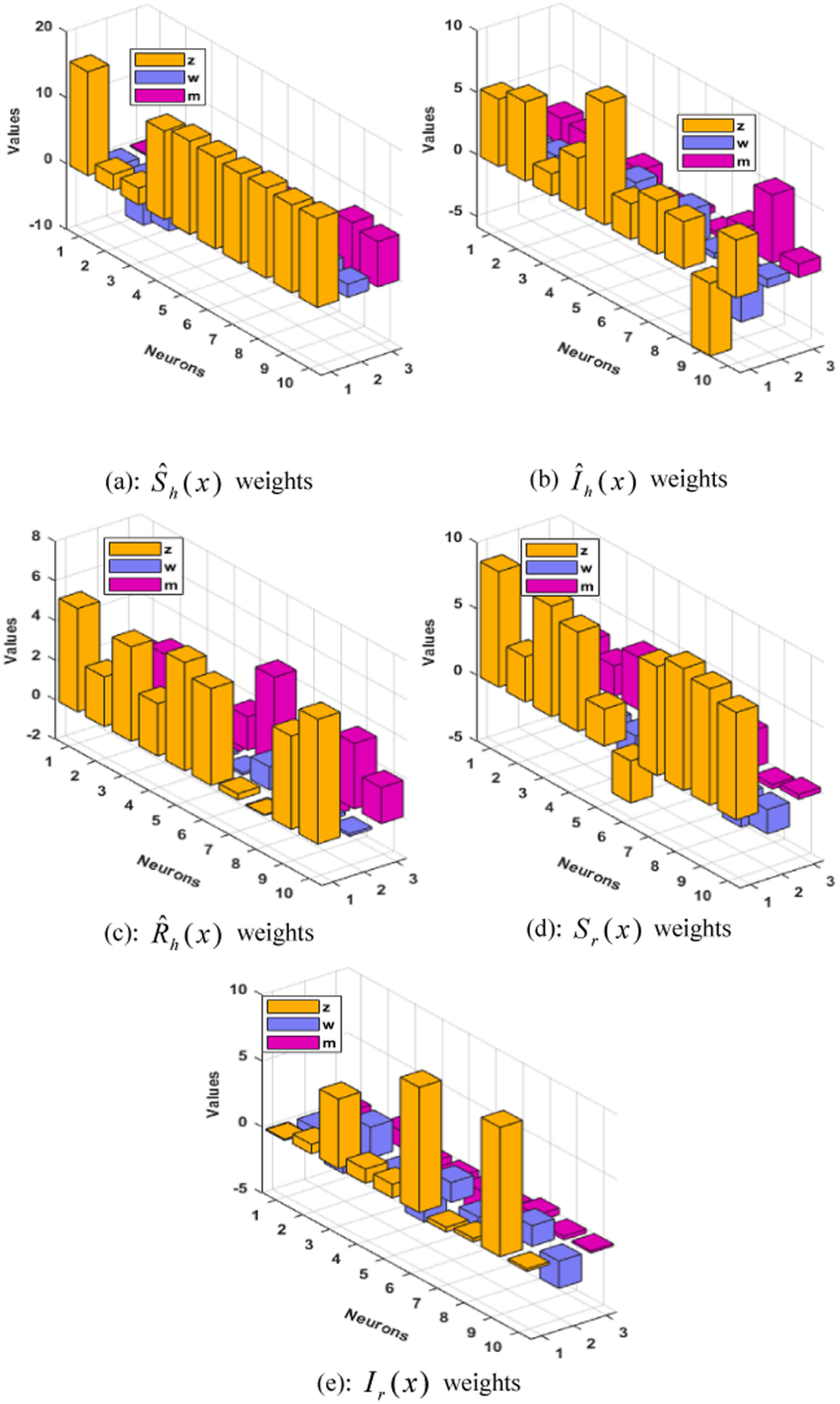

Fig. 2. Optimal weight vectors using the Meyer WNN for solving the LDM.

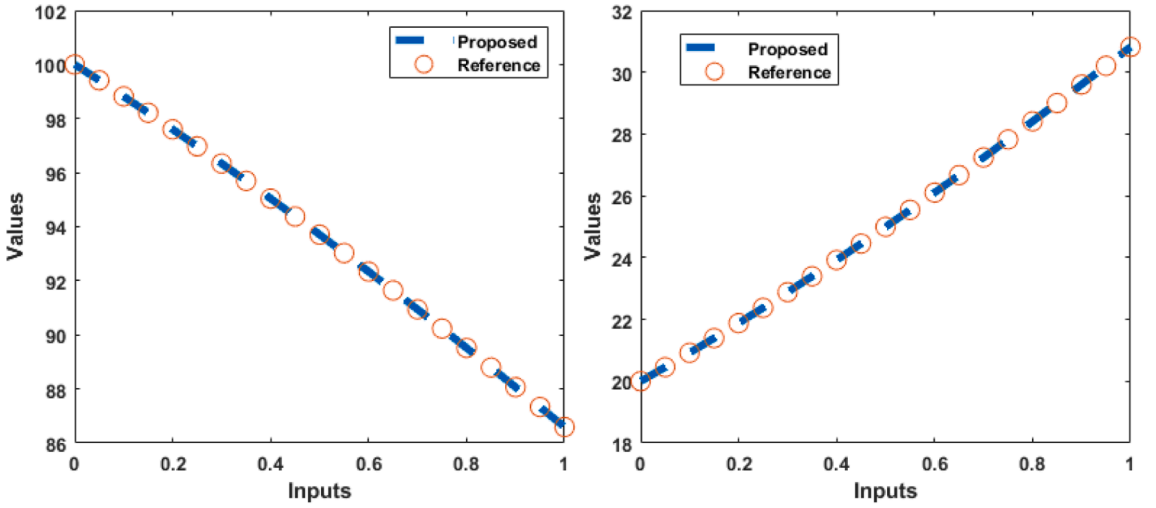

(a): Comparison of first class

(b) Comparison of second class

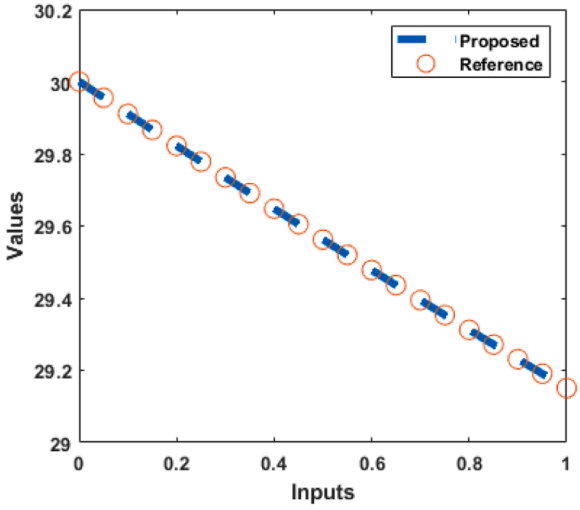

(c): Comparison of third class

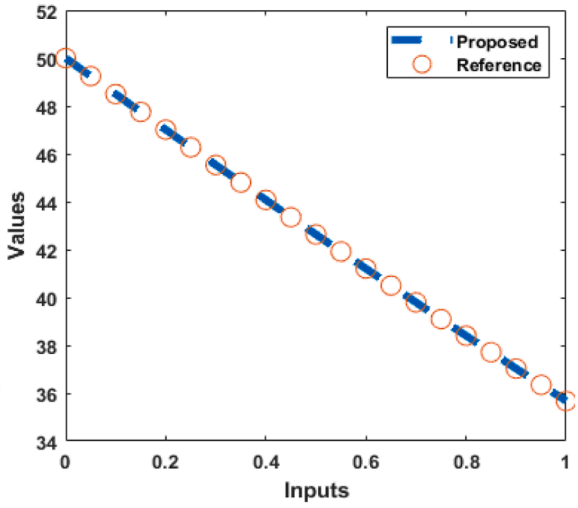

(d): Comparison of fourth class

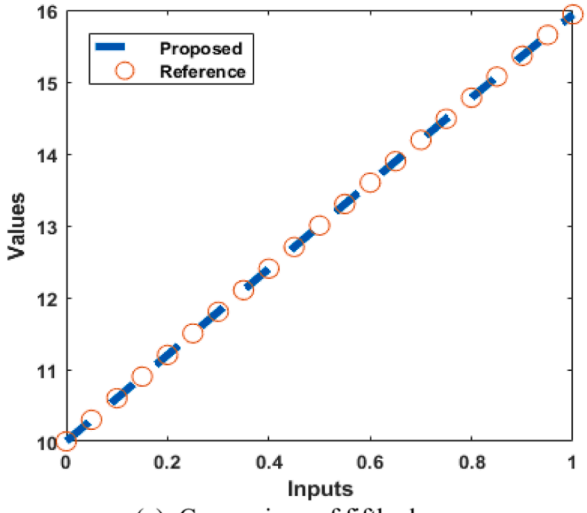

(e): Comparison of fifth class

Fig. 3. Comparison performances based each category of the LDM.

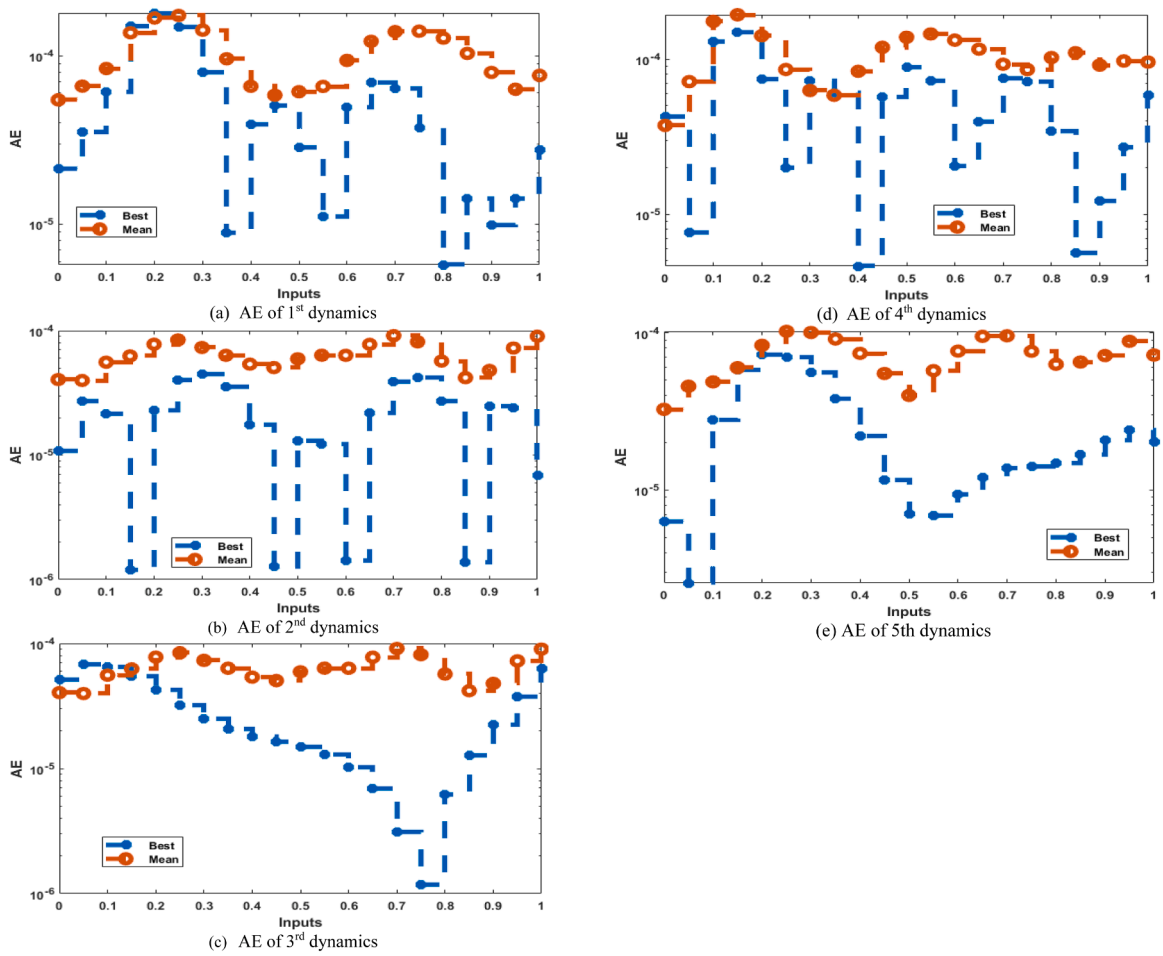

Fig. 4. The values of the AE using the Meyer WNN to solve the LDM.

on the TIC and EVAF measures have determined around 10^{-08} to 10^{-09}, and 10^{-09} to 10^{-11} for each dynamic of the LDM. These achieved performances of the results are calculated adequately for each class of the LDM by applying the procedures of Meyer WNN along with the GAASA.

To perform the accurateness of the procedure, the statistical observations for different statistical values have been shown in Tables 2-4 to solve the LDM. The statistical performances based on the Minimum (Min), S-I-R, Maximum (Max), standard deviation (STD), and Median (MD) have been tabulated in these analyses. The Max and Min observations signify the worst and best results using ten numbers of executions. For the respective categories of the LDM, the Min, S-I-R, Max, STD, and MD measures provide good measure. One can observe that these small achieved performances are accurate (Tables 5 and 6).

4. Final remarks

In this work, a novel design of a Meyer wavelet neural network is presented for solving the mathematical form of the Leptospirosis disease model. Leptospirosis is an infection spread by rodents, which is found in the world and causes fatalities in humans. The nonlinear form of the Leptospirosis model is consistent on susceptible, infected, and recovered dynamics including two more class based on the population of vector (rat) and human. Some concluding remarks of this study are presented as:

- A novel design through the Meyer wavelet neural network has been proposed successfully for solving the mathematical Leptospirosis model.
- A merit function has been designed based on the differential form of the Leptospirosis model and its initial conditions.
- The optimization of the merit function has been performed through the global and local search optimization schemes using the genetic algorithm and active-set algorithm to solve the Leptospirosis model.
- The comparison of the results provides the correctness of the proposed Meyer wavelet neural network scheme.
- The small calculated absolute error that is around 10^{-06} to 10^{-07} presents the effectiveness of the scheme.
- The reliability is authenticated through different statistical operator's performances by taking 20 numbers of trials.

The proposed Meyer WNN scheme can be used in future studies for the numerical solutions of the different differential systems (Barboteu

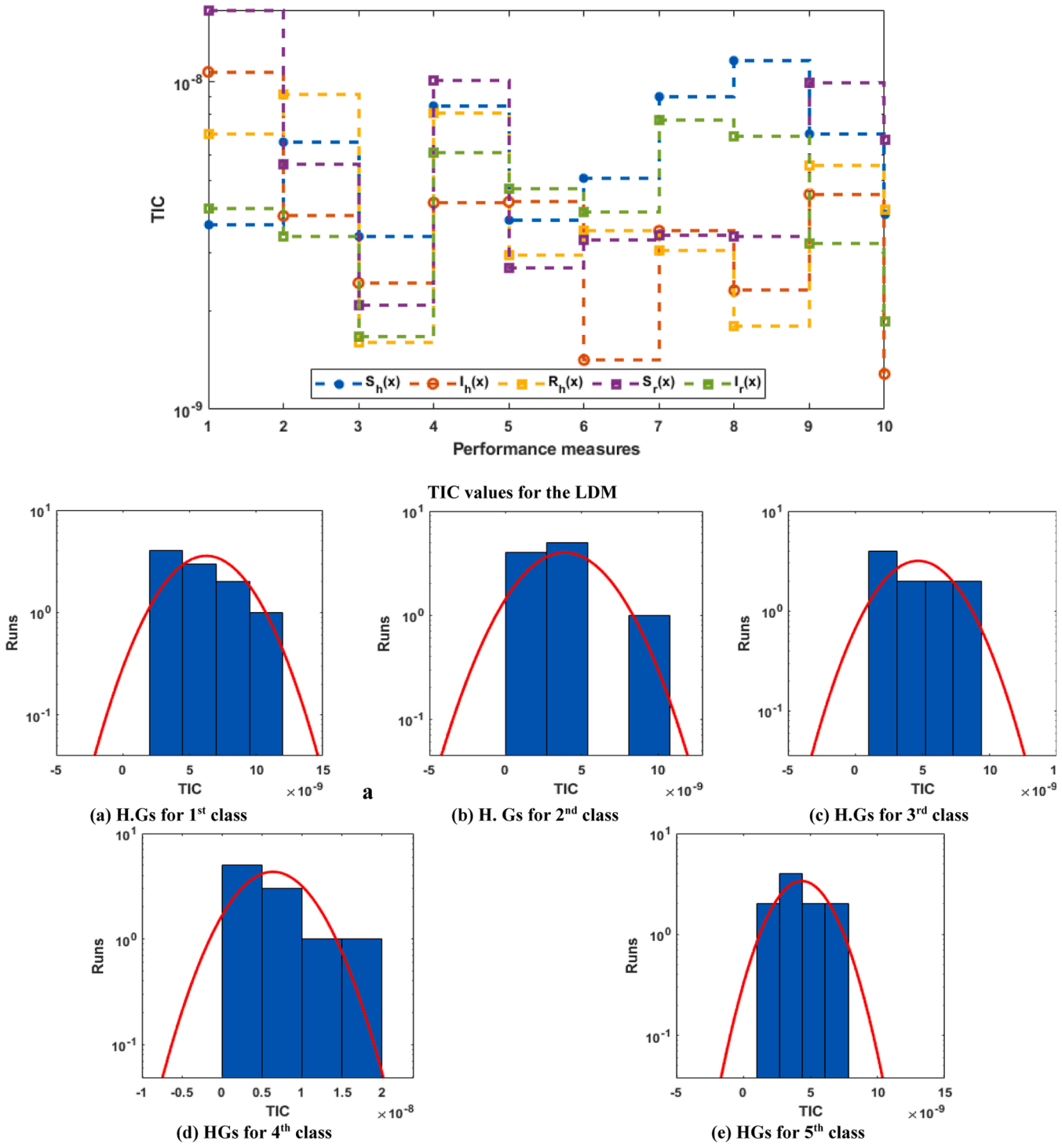

Fig. 5. Convergence of TIC operators using the Meyer WNN to solve the LDM.

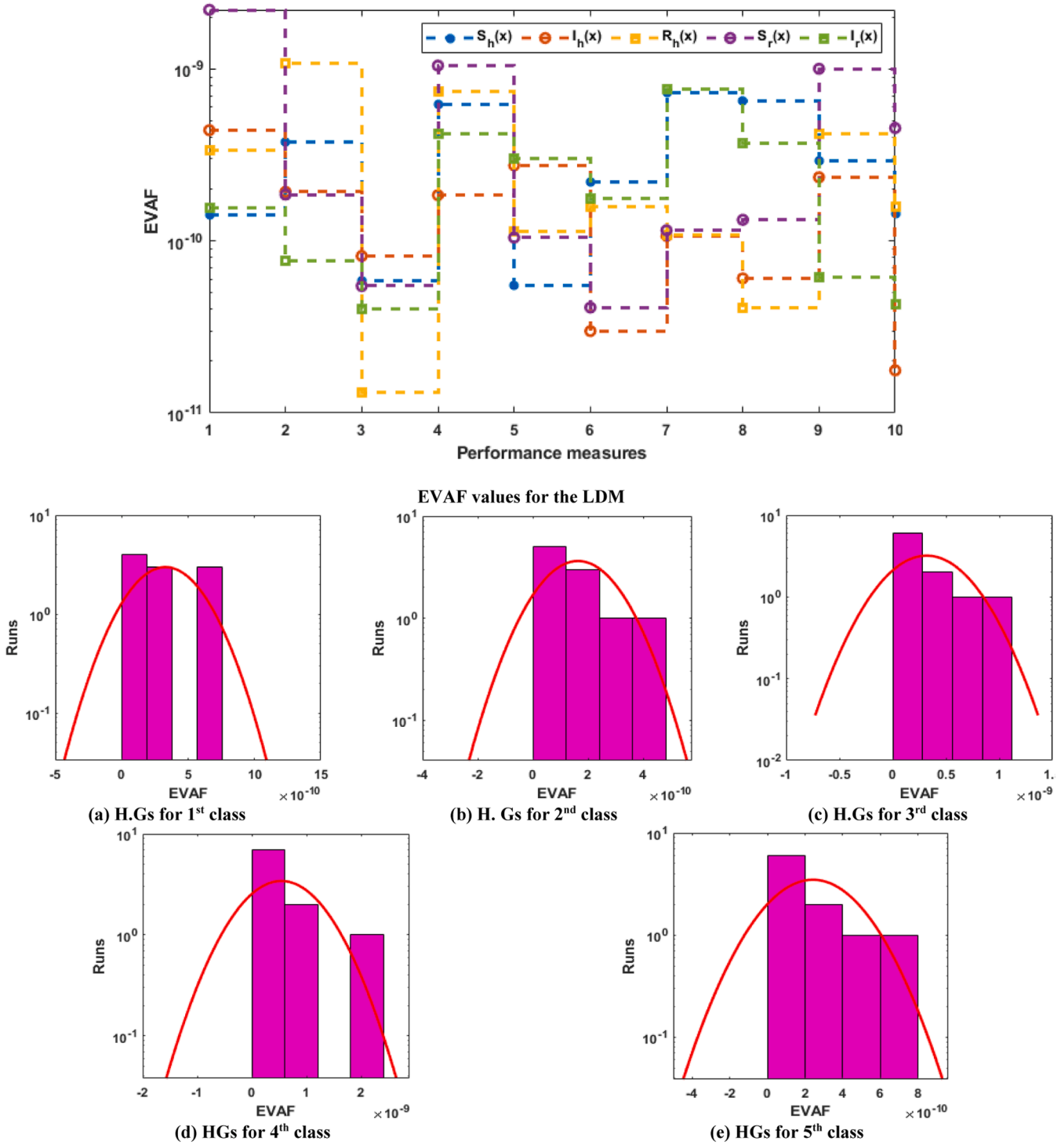

Fig. 6. Convergence of EVAF operators using the Meyer WNN to solve the LDM.

Table 2
Statistical representations of LDM for first category.

x	Min	S-I-R	Max	STD	MD
0	5.20659E-06	2.63596E-05	2.65561E-04	7.88779E-05	5.46616E-05
0.05	5.44833E-06	9.58327E-06	3.66927E-04	1.06945E-04	6.59346E-05
0.1	5.50092E-06	3.88365E-05	2.67854E-04	7.36184E-05	8.38748E-05
0.15	2.46447E-07	2.90597E-05	2.38830E-04	6.28853E-05	1.36797E-04
0.2	2.49365E-05	6.08350E-05	3.29152E-04	9.64722E-05	1.67341E-04
0.25	6.30980E-05	7.88769E-05	3.62168E-04	9.90091E-05	1.73328E-04
0.3	3.87703E-06	7.38449E-05	3.36198E-04	9.91057E-05	1.41799E-04
0.35	8.88024E-06	6.16058E-05	2.67747E-04	8.51568E-05	9.58814E-05
0.4	5.84936E-06	3.58068E-05	1.82766E-04	5.54893E-05	6.57890E-05
0.45	5.67356E-06	2.52899E-05	1.36269E-04	4.17417E-05	5.82687E-05
0.5	1.03886E-05	1.99361E-05	2.09471E-04	5.88583E-05	6.11196E-05
0.55	9.47939E-07	3.04107E-05	2.47065E-04	7.91594E-05	6.57048E-05
0.6	9.49394E-08	3.83940E-05	2.43914E-04	7.30403E-05	9.37369E-05
0.65	2.87497E-05	5.41682E-05	2.06213E-04	6.59990E-05	1.21726E-04
0.7	4.90759E-05	5.80320E-05	2.77943E-04	8.39132E-05	1.38940E-04
0.75	2.45115E-05	6.36060E-05	3.36035E-04	1.13389E-04	1.39756E-04
0.8	5.73563E-06	7.04367E-05	3.46272E-04	1.23844E-04	1.27234E-04
0.85	2.73641E-07	6.34638E-05	2.97529E-04	1.04679E-04	1.03223E-04
0.9	9.85405E-06	4.86826E-05	2.05209E-04	6.01116E-05	7.95860E-05
0.95	1.13038E-05	4.49961E-05	1.47661E-04	4.97728E-05	6.32403E-05
1	2.65849E-05	5.07435E-05	1.56782E-04	5.22666E-05	7.63837E-05

Table 3
Statistical representations of LDM for second category.

x	Min	S-I-R	Max	STD	MD
0	1.74462E-06	1.90802E-05	1.56640E-04	4.59437E-05	4.04763E-05
0.05	1.64208E-06	2.16310E-05	1.53037E-04	4.77296E-05	3.97927E-05
0.1	1.02409E-05	1.93438E-05	2.21837E-04	6.12253E-05	5.58306E-05
0.15	1.19746E-06	3.95115E-05	2.88539E-04	8.59974E-05	6.26107E-05
0.2	1.36142E-06	3.44329E-05	3.13775E-04	9.03805E-05	7.77707E-05
0.25	2.85497E-05	3.60991E-05	2.89202E-04	8.14359E-05	8.42797E-05
0.3	2.23358E-06	1.51947E-05	2.28903E-04	7.09168E-05	7.32491E-05
0.35	1.01732E-05	2.57408E-05	1.58848E-04	5.06346E-05	6.33496E-05
0.4	6.41126E-06	3.47474E-05	1.30435E-04	4.58799E-05	5.37980E-05
0.45	1.27093E-06	4.30084E-05	1.67238E-04	5.58322E-05	5.04856E-05
0.5	1.57443E-06	5.13859E-05	1.57750E-04	5.49641E-05	5.94060E-05
0.55	7.57544E-06	4.09798E-05	1.72915E-04	5.65703E-05	6.34671E-05
0.6	1.41602E-06	4.29668E-05	2.38907E-04	7.37894E-05	6.33660E-05
0.65	8.07331E-06	4.02707E-05	2.85587E-04	8.50746E-05	7.76136E-05
0.7	3.40791E-06	2.63434E-05	2.91697E-04	8.17410E-05	9.12145E-05
0.75	5.56125E-06	3.14475E-05	2.51159E-04	7.04799E-05	8.13393E-05
0.8	3.60562E-06	2.26648E-05	1.81744E-04	5.46915E-05	5.69882E-05
0.85	1.38334E-06	4.86507E-05	1.20741E-04	4.82685E-05	4.18872E-05
0.9	5.38793E-06	4.12575E-05	1.10745E-04	4.23348E-05	4.79438E-05
0.95	1.39837E-05	3.98488E-05	1.75985E-04	5.86613E-05	7.25623E-05
1	6.82634E-06	6.87324E-05	2.04713E-04	7.23444E-05	9.01725E-05

Table 4
Statistical representations of LDM for third category.

x	Min	S-I-R	Max	STD	MD
0	4.55315E-08	9.05113E-06	5.16536E-05	1.56186E-05	1.48065E-05
0.05	8.57493E-06	2.64700E-05	9.83425E-05	3.15718E-05	4.82979E-05
0.1	9.28612E-06	2.73837E-05	1.35221E-04	4.33299E-05	5.32202E-05
0.15	7.34181E-06	2.14469E-05	1.48543E-04	4.28987E-05	4.55030E-05
0.2	5.90939E-06	2.36902E-05	1.44547E-04	4.86197E-05	5.30379E-05
0.25	3.69053E-06	3.61283E-05	2.32598E-04	6.80371E-05	7.34678E-05
0.3	2.50798E-05	6.62564E-05	2.86025E-04	8.41168E-05	9.81521E-05
0.35	4.27397E-06	7.68058E-05	2.96904E-04	9.85566E-05	1.13672E-04
0.4	1.80964E-05	7.67497E-05	2.98866E-04	9.59247E-05	1.28234E-04
0.45	1.64923E-05	4.83584E-05	3.29434E-04	8.95841E-05	1.32532E-04
0.5	1.49669E-05	2.01429E-05	3.32689E-04	8.53626E-05	1.26445E-04
0.55	1.29731E-05	5.09069E-05	3.09024E-04	8.53427E-05	1.11799E-04
0.6	1.02971E-05	3.59481E-05	2.61316E-04	7.79594E-05	9.82774E-05
0.65	6.96297E-06	2.90397E-05	2.07277E-04	6.85655E-05	8.36552E-05
0.7	3.12222E-06	3.32876E-05	2.07093E-04	6.08738E-05	6.62684E-05
0.75	1.18189E-06	1.51477E-05	1.96285E-04	5.41810E-05	5.08181E-05
0.8	2.11495E-06	1.51553E-05	1.76368E-04	5.37241E-05	4.33988E-05
0.85	5.30293E-06	4.06609E-05	1.49564E-04	5.15070E-05	5.77221E-05
0.9	2.98014E-06	4.85104E-05	1.75586E-04	5.94451E-05	6.70360E-05
0.95	4.30292E-06	3.19531E-05	2.14478E-04	6.28873E-05	6.34773E-05
1	2.73554E-06	2.29873E-05	1.64438E-04	4.68937E-05	4.84259E-05

Table 5
Statistical representations of LDM for fourth category.

x	Min	S-I-R	Max	STD	MD
0	2.28070E-06	1.92937E-05	1.16685E-04	3.47065E-05	3.73936E-05
0.05	7.64739E-06	3.21159E-05	2.90394E-04	8.27841E-05	7.16359E-05
0.1	6.23816E-05	5.39475E-05	4.97218E-04	1.29069E-04	1.75410E-04
0.15	5.35531E-05	9.78860E-05	4.28418E-04	1.29795E-04	1.93361E-04
0.2	1.19439E-05	1.08972E-04	3.12522E-04	1.17257E-04	1.41586E-04
0.25	4.35126E-06	7.20541E-05	2.54092E-04	9.02984E-05	8.57565E-05
0.3	5.46305E-06	3.11247E-05	1.45965E-04	4.93973E-05	6.27753E-05
0.35	6.17024E-06	1.42025E-05	2.84045E-04	8.09204E-05	5.84791E-05
0.4	2.70650E-06	2.59001E-05	4.45347E-04	1.30418E-04	8.35328E-05
0.45	4.99839E-05	1.90505E-05	5.15056E-04	1.41019E-04	1.19160E-04
0.5	6.81900E-05	3.77648E-05	4.54453E-04	1.17621E-04	1.38391E-04
0.55	3.05774E-05	7.88529E-05	2.99390E-04	9.16684E-05	1.45401E-04
0.6	7.34387E-06	4.15997E-05	3.56613E-04	1.13970E-04	1.32445E-04
0.65	2.08840E-05	5.14493E-05	3.73589E-04	1.16292E-04	1.15932E-04
0.7	6.18605E-07	6.21971E-05	2.62717E-04	8.48175E-05	9.27189E-05
0.75	4.09415E-06	2.50209E-05	2.64759E-04	7.14307E-05	8.56419E-05
0.8	4.97769E-06	3.56922E-05	4.38695E-04	1.24110E-04	1.02356E-04
0.85	5.61771E-06	4.48184E-05	5.07906E-04	1.48539E-04	1.09924E-04
0.9	1.21104E-05	3.73157E-05	3.95605E-04	1.12262E-04	9.15035E-05
0.95	1.82654E-05	5.79225E-05	2.19511E-04	7.27395E-05	9.73111E-05
1	6.90527E-06	2.54523E-05	2.36431E-04	7.59566E-05	9.57622E-05

Table 6
Statistical representations of LDM for fifth category.

x	Min	S-I-R	Max	STD	MD
0	9.90586E-05	1.96301E-05	9.90586E-05	2.98653E-05	3.25872E-05
0.05	1.38207E-04	4.56266E-05	1.38207E-04	4.99672E-05	4.56579E-05
0.1	9.67829E-05	2.70933E-05	9.67829E-05	3.07156E-05	4.86896E-05
0.15	1.44274E-04	1.38608E-05	1.44274E-04	4.72608E-05	5.99331E-05
0.2	1.73292E-04	6.70998E-05	1.73292E-04	6.55350E-05	8.31082E-05
0.25	2.29104E-04	4.85193E-05	2.29104E-04	7.17975E-05	1.01990E-04
0.3	2.72130E-04	2.16331E-05	2.72130E-04	8.44847E-05	1.00242E-04
0.35	2.77441E-04	2.98469E-05	2.77441E-04	8.39467E-05	9.12146E-05
0.4	2.48323E-04	3.41159E-05	2.48323E-04	7.33448E-05	7.38813E-05
0.45	1.93781E-04	1.80782E-05	1.93781E-04	5.26424E-05	5.50424E-05
0.5	1.25877E-04	2.62193E-05	1.25877E-04	4.31461E-05	3.99421E-05
0.55	1.53965E-04	3.03594E-05	1.53965E-04	4.58281E-05	5.73663E-05
0.6	1.96308E-04	6.08985E-05	1.96308E-04	6.58838E-05	7.63806E-05
0.65	2.22651E-04	5.97125E-05	2.22651E-04	6.78297E-05	9.47682E-05
0.7	2.24045E-04	3.86510E-05	2.24045E-04	6.11856E-05	9.55158E-05
0.75	1.93274E-04	4.07269E-05	1.93274E-04	5.86572E-05	7.61477E-05
0.8	1.49672E-04	3.43631E-05	1.49672E-04	4.68636E-05	6.29566E-05
0.85	1.34479E-04	4.30820E-05	1.34479E-04	4.42273E-05	6.51020E-05
0.9	1.83330E-04	3.57335E-05	1.83330E-04	6.30911E-05	7.15316E-05
0.95	2.04837E-04	4.67184E-05	2.04837E-04	6.82753E-05	8.81451E-05
1	1.62036E-04	4.47007E-05	1.62036E-04	4.97536E-05	7.20773E-05

and Dumont, 2018, Baskonus et al., 2019, Barapatre et al., 2022, Roshni and Musthafa, 2022, Yokuş and Gülbahar, 2019, Dewasurendra and Vajravelu, 2018, Günerhan and Çelik, 2020, Dharmik et al., 2022, Pokle et al., 2022, Sulaiman et al., 2021, Gençoğlu and Agarwal, 2021).

CRediT authorship contribution statement

Zulqurnain Sabir: Data curation, Writing – original draft. **Muhammad Asif Zahoor Raja:** Visualization, Investigation. **Mohamed R. Ali:** Software, Validation, Writing – review & editing. **R. Sadat:** Conceptualization, Methodology, Software. **Irwan Fathurrochman:** . **Rafaél Artidoro Sandoval Núñez:** . **Shahid Ahmad Bhat:** Supervision.

Declaration of Competing Interest

The authors declare that they have no known competing financial interests or personal relationships that could have appeared to influence the work reported in this paper.

Data availability

Data will be made available on request.

References

Abide, S., Barboteu, M., Cherkaoui, S., & Dumont, S. (2021). A semi-smooth Newton and Primal–Dual Active Set method for Non-Smooth Contact Dynamics. *Computer Methods in Applied Mechanics and Engineering, 387*, Article 114153.

Americo, J. L., Earl, P. L., & Moss, B. (2023). Virulence differences of mpox (monkeypox) virus clades I, IIa, and IIb. 1 in a small animal model. *Proceedings of the National Academy of Sciences, 120*(8), Article e2220415120.

Barapatre, P., Ingolikar, Y., Desai, P., Jajoo, P., & Thakre, P. (2022). A secured architecture for iot-based healthcare system. *3c Empresa: Investigación y Pensamiento Crítico, 11*(2), 222–230.

Barboteu, M., & Dumont, S. (2018). A primal-dual active set method for solving multi-rigid-body dynamic contact problems. *Mathematics and Mechanics of Solids, 23*(3), 489–503.

Baskonus, H. M., Bulut, H., & Sulaiman, T. A. (2019). New complex hyperbolic structures to the lonngren-wave equation by using sine-gordon expansion method. *Applied Mathematics and Nonlinear Sciences, 4*(1), 129–138.

Bhadauria, A. S., Pathak, R., & Chaudhary, M. (2021). A SIQ mathematical model on COVID-19 investigating the lockdown effect. *Infectious Disease Modelling, 6*, 244–257.

Bhalraj, A., & Azmi, A. (2019). Mathematical modelling of the spread of Leptospirosis. In *, 2184*. *AIP Conference Proceedings*. AIP Publishing LLC, Article 060031.
Bhalraj, A., Azmi, A., & Mohd, M. H. (2021). Analytical and numerical solutions of Leptospirosis Model. *Computer Science, 16*(3), 949–961.
Deuerlein, J. W., Piller, O., Elhay, S., & Simpson, A. R. (2019). Content-based active-set method for the pressure-dependent model of water distribution systems. *Journal of Water Resources Planning and Management, 145*(1), Article 04018082.
Dewasurendra, M., & Vajravelu, K. (2018). On the method of inverse mapping for solutions of coupled systems of nonlinear differential equations arising in nanofluid flow, heat and mass transfer. *Applied Mathematics and Nonlinear Sciences, 3*(1), 1–14.
Dharmik, R. C., Chavhan, S., & Sathe, S. R. (2022). Deep Learning based missing object Detection and Person Identification: An application for Smart CCTV. *3c Tecnología: Glosas de Innovación Aplicadas a la Pyme, 11*(2), 51–57.
El-Shahed, M. (2014). Fractional order model for the spread of leptospirosis. *International Journal of Mathematical Analysis, 8*(54), 2651–2667.
El-Shorbagy, M. A., Ayoub, A. Y., Mousa, A. A., & El-Desoky, I. M. (2019). An enhanced genetic algorithm with new mutation for cluster analysis. *Computational statistics, 34*, 1355–1392.
Gençoğlu, M. T., & Agarwal, P. (2021). Use of quantum differential equations in sonic processes. *Applied Mathematics and Nonlinear Sciences, 6*(1), 21–28.
Goh, S. H., Ismail, R., Lau, S. F., Megat Abdul Rani, P. A., Mohd Mohidin, T. B., Daud, F., Bahaman, A. R., Khairani-Bejo, S., Radzi, R., & Khor, K. H. (2019). Risk factors and prediction of leptospiral seropositivity among dogs and dog handlers in Malaysia. *International Journal of Environmental Research and Public Health, 16*(9), 1499.
Guerrero Sánchez, Y., Sabir, Z., Günerhan, H., & Baskonus, H. M. (2020). Analytical and approximate solutions of a novel nervous stomach mathematical model. *Discrete Dynamics in Nature and Society, 2020*.
Günerhan, H., & Çelik, E. (2020). Analytical and approximate solutions of fractional partial differential-algebraic equations. *Applied Mathematics and Nonlinear Sciences, 5*(1), 109–120.
He, X., & Yang, P. (2019). The primal-dual active set method for a class of nonlinear problems with-monotone operators. *Mathematical Problems in Engineering, 2019*.
Huo, W., Li, W., Sun, C., Ren, Q., & Gong, G. (2022). Research on fuel cell fault diagnosis based on genetic algorithm optimization of support vector machine. *Energies, 15*(6), 2294.
Keeling, M. (2001). The mathematics of diseases. *Plus Magazine, 14*.
Keeling, M. J., & Rohani, P. (2011). *Modeling infectious diseases in humans and animals*. Princeton University Press.
Khan, M. A., Saddiq, S. F., Islam, S., Khan, I., & Shafie, S. (2016). Dynamic behavior of leptospirosis disease with saturated incidence rate. *International Journal of Applied and Computational Mathematics, 2*(4), 435–452.
Khan, M. F., Alrabaiah, H., Ullah, S., Khan, M. A., Farooq, M., bin Mamat, M., & Asjad, M. I. (2021). A new fractional model for vector-host disease with saturated treatment function via singular and non-singular operators. *Alexandria Engineering Journal, 60*(1), 629–645.
Khan, P. W., Yeun, C. Y., & Byun, Y. C. (2023). Fault detection of wind turbines using SCADA data and genetic algorithm-based ensemble learning. *Engineering Failure Analysis, 148*, Article 107209.
Kongnuy, R. (2012). Local Stability of Equilibria: Leptospirosis. *International Journal of Mathematical and Computational Sciences, 6*(6), 625–629.
Liang, H., Zou, J., Zuo, K., & Khan, M. J. (2020). An improved genetic algorithm optimization fuzzy controller applied to the wellhead back pressure control system. *Mechanical Systems and Signal Processing, 142*, Article 106708.
Lim, J. K., Murugaiyah, V. A., Ramli, A. S., Rahman, H. A., Mohamed, N. S. F., Shamsudin, N. N., & Tan, J. C. (2011). *A case study: Leptospirosis in Malaysia*.
Peter, O. J., Kumar, S., Kumari, N., Oguntolu, F. A., Oshinubi, K., & Musa, R. (2021). Transmission dynamics of Monkeypox virus: a mathematical modelling approach. *Modeling Earth Systems and Environment*, 1–12.
Pokle, S., Deshpande, R., Paraskar, S., Sinha, S., Lalwani, Y., & Thakre, P. N. (2022). Performance analysis of NOMA in Rayleigh and Nakagami Fading channel. *3 c TIC: Cuadernos de Desarrollo Aplicados a Las TIC, 11*(2), 183–193.
Quirynen, R., Knyazev, A., & Di Cairano, S. (2018). Block structured preconditioning within an active-set method for real-time optimal control. In *2018 European Control Conference (ECC)* (pp. 1154–1159). IEEE.
Roshni, K. S., & Musthafa, M. M. A. (2022). Problems of online mathematics teaching and learning during the pandemic: A reverberation in to the perception of prospective teachers. *3c Empresa: Investigación y Pensamiento Crítico, 11*(2), 153–162.
Sabir, Z., et al. (2020). A neuro-swarming intelligence based computing for second order singular periodic nonlinear boundary value problems. *Frontiers in Physics, 8*, 224. https://doi.org/10.3389/fphy.2020.00224
Sabir, Z. (2022). Neuron analysis through the swarming procedures for the singular two-point boundary value problems arising in the theory of thermal explosion. *The European Physical Journal Plus, 137*(5), 638.
Sabir, Z. (2022). Stochastic numerical investigations for nonlinear three-species food chain system. *International Journal of Biomathematics, 15*(04), Article 2250005.
Sabir, Z., Sadat, R., Ali, M. R., Said, S. B., & Azhar, M. (2023). A numerical performance of the novel fractional water pollution model through the Levenberg-Marquardt backpropagation method. *Arabian Journal of Chemistry, 16*(2), Article 104493.
Sabir, Z., Umar, M., Raja, M. A. Z., & Baleanu, D. (2021). Applications of Gudermannian neural network for solving the SITR fractal system. *Fractals*.
Sabir, Z., Umar, M., Raja, M. A. Z., Fathurrochman, I., & Hasan, H. (2022). Design of Morlet wavelet neural network to solve the non-linear influenza disease system. *Applied Mathematics and Nonlinear Sciences*.
Sánchez, Y. G., Sabir, Z., & Guirao, J. L. (2020). Design of a nonlinear SITR fractal model based on the dynamics of a novel coronavirus (COVID-19). *Fractals, 28*(08), Article 2040026.
Sathya, M., Jeyaselvi, M., Joshi, S., Pandey, E., Pareek, P. K., Jamal, S. S., Kumar, V., & Atiglah, H. K. (2022). Cancer categorization using genetic algorithm to identify biomarker genes. *Journal of Healthcare Engineering, 2022*.
Shanmugasundaram, N., Sushita, K., Kumar, S. P., & Ganesh, E. N. (2019). Genetic algorithm-based road network design for optimising the vehicle travel distance. *International Journal of Vehicle Information and Communication Systems, 4*(4), 344–354.
Song, H., Wang, X., Zhang, K., & Zhang, Q. (2017). Primal-dual active set method for American lookback put option pricing. *East Asian Journal on Applied Mathematics, 7*(3), 603–614.
Sulaiman, T. A., Bulut, H., & Baskonus, H. M. (2021). On the exact solutions to some system of complex nonlinear models. *Applied Mathematics and Nonlinear Sciences, 6*(1), 29–42.
Thayaparan, S., Robertson, I. D., Fairuz, A., Suut, L., & Abdullah, M. T. (2013). Leptospirosis, an emerging zoonotic disease in Malaysia. *Malaysian Journal of Pathology, 35*(2), 123–132.
Triampo, W., Baowan, D., Tang, I. M., Nuttavut, N., Wong-Ekkabut, J., & Doungchawee, G. (2007). A simple deterministic model for the spread of leptospirosis in Thailand. *International Journal of Biomedical Science, 2*, 22–26.
Umar, M (2020). A stochastic computational intelligent solver for numerical treatment of mosquito dispersal model in a heterogeneous environment. *The European Physical Journal Plus, 135*(7), 1–23.
Umar, M., et al. (2019). Unsupervised constrained neural network modeling of boundary value corneal model for eye surgery. *Applied Soft Computing, 85*, Article 105826.
Umar, M., et al. (2019). Intelligent computing for numerical treatment of nonlinear prey–predator models. *Applied Soft Computing, 80*, 506–524.
Umar, M., et al. (2020). Stochastic numerical technique for solving HIV infection model of CD4+ T cells. *The European Physical Journal Plus, 135*(6), 403.
Umar, M., Sabir, Z., Raja, M. A. Z., & Sánchez, Y. G. (2020). A stochastic numerical computing heuristic of SIR nonlinear model based on dengue fever. *Results in Physics, 19*, Article 103585.
Wang, H., Lang, X., & Mao, W. (2021). Voyage optimization combining genetic algorithm and dynamic programming for fuel/emissions reduction. *Transportation Research Part D: Transport and Environment, 90*, Article 102670.
Wang, Z., Cao, L., & Si, H. (2021). An improved genetic algorithm for determining the optimal operation strategy of thermal energy storage tank in combined heat and power units. *Journal of Energy Storage, 43*, Article 103313.
Yang, Y., Yang, B., Wang, S., Liu, F., Wang, Y., & Shu, X. (2019). A dynamic ant-colony genetic algorithm for cloud service composition optimization. *The International Journal of Advanced Manufacturing Technology, 102*, 355–368.
Yarsky, P. (2021). Using a genetic algorithm to fit parameters of a COVID-19 SEIR model for US states. *Mathematics and Computers in Simulation, 185*, 687–695.
Yokuş, A., & Gülbahar, S. (2019). Numerical solutions with linearization techniques of the fractional Harry Dym equation. *Applied Mathematics and Nonlinear Sciences, 4*(1), 35–42.